

# Near vs far field: interference aggregation in TV whitespaces

## Extended Edition

Kristen Woyach, Pulkit Grover, and Anant Sahai  
Department of EECS, UC Berkeley  
{kwoyach, pulkit, sahai}@eecs.berkeley.edu

**Abstract**—We investigate the behavior of aggregate interference in a model applicable to cognitive radios. We find that a behavioral phase change occurs depending on the relationship between the distance between whitespace devices and the distance from these devices to the primary receiver. For a model where cognitive transmitters are placed deterministically on a grid, the mean of the interference behaves differently depending on whether the problem is one of “near field” or “far field”. When these transmitters are placed randomly, the shape of the distribution changes from a heavy-tailed distribution to something that is approximately Gaussian in moving from near field towards far field. These behavioral changes suggest that in designing rules for whitespace devices, the FCC rules may have to be sensitive to whether the situation is one of near field or far field.

### I. INTRODUCTION

The FCC, in its whitespace rulings, [1], [2] has adopted a “one size fits all” approach to interference mitigation between whitespace devices and TV receivers: the whitespace devices must remain 14.4 km away from the protected region of TV receivers, the so-called “no-talk zone”. Outside this range, there is a per-node power limitation, but no restriction on the density of transmitters. In [3], the authors note that the U.S. has a wide range of densities of people outside the no-talk zone, depending on whether the region of interest is in a rural or urban area. Therefore there will likely also be a large range of how many whitespace devices are operating. Broadly, in this paper, we are interested in exploring the following question: can *any* “one-size fits all” rule work well for *all* densities?

The government regulator is using this rule to guarantee that the primary will experience too much interference only a small fraction of the time. To achieve this goal, what *should* the placement and power-control rules look like? In [3], the authors show that if a reasonable fraction of the people outside the no-talk zone have whitespace devices, the total aggregate interference coming from these devices can be enough to disrupt TV service for protected TV receivers. This is shown with a deterministic placement of nodes (on a grid) and a deterministic propagation model.

Results of [3] provide one approach based on limiting the power density outside the no-talk radius. In [4], [5], Hoven

*et al.* provide another rule with bounds on what the no-talk radius must be for a “one-size-fits-all” rule to work. The model for the placement of whitespace devices is a sea (*i.e.* a continuum of infinitely-small devices) outside the no-talk radius, and fading is included. In [6], Nguyen and Baccelli use the aggregate interference calculations from [7] to look at the coverage probability with *random placement* (according to a 2D Poisson model) of primary and secondaries. In [8], the same authors use these Poisson models to understand the effect of the aggregate interference on the coverage probability of TV transmitters.<sup>1</sup>

In this paper, we help inform the problem of developing rules by taking a closer look at how the aggregate interference behaves for different placement models with and without fading. We focus on two situations: “near-field” and “far-field” to see whether different situations require different rules. Traditionally, the definitions of near and far field depend on the context: in electromagnetics, they refer to the distance between transmitter and receiver relative to the wavelength [9]. For interference calculations, in [7], these terms refer to the *distance between the interferers* (call this  $d$ ) relative to the distance of the *interferers to the receiver experiencing the interference* (call this  $r_n$ ). Is this definition also appropriate for cognitive radio problems? In essence, near and far field can be distinguished by a behavioral phase change that occurs with distance. We show in this paper that for cognitive radios, such a phase-change does happen, and indeed depends on  $d$  and  $r_n$ . More precisely, near field is when  $d \gg r_n$  and far field is when  $d \ll r_n$ .

In this paper, we use techniques from spatial networks (see for example [7], [10]–[14]) to demonstrate and explore the behavioral phase change that occurs when  $d$  and  $r_n$  change. We show in Section III that even with deterministic placement in a grid model (like that in [10]), near and far field exhibit different rates of decay of aggregate interference with  $r_n$ . We then move in Section IV to a Poisson placement model [7]. Here, we observe that the behavior of the mean and variance does *not* vary with near and far field. However, the *distribution* of the interference is very different: in near field, the distribution exhibits heavy tails, but in far field,

We would like to thank Francois Baccelli for introducing us to the Stochastic Geometry tools used in this paper and for the conversations that began these investigations.

<sup>1</sup>The literature for aggregate interference is extensive. We are trying to extend the stochastic geometry part of this literature, and so we have cited only the most relevant papers. We will include a wider literature search in the final version.

the distribution of interference converges to a (lighter-tailed) Gaussian and concentrates around the mean.

If the effect of adding random placement significantly changes the impact of being in near or far field, what happens when we include additional real-world randomness of channel-fading [15]? In Section V, we show that fading increases the variance and slows the convergence to Gaussian. So, fading exaggerates the effect of near field and extends the range of parameters included in the near field. But, it does *not* change the qualitative behavior of interference distribution in near or far field.

Finally, in Section VI, we discuss what these results mean for a government regulator trying to define operational rules for whitespace devices. In particular, we show that practical situations can correspond to both near and far fields, and thus extra care might be required to design rules for situations that correspond to near field.

## II. NOTATION, DEFINITIONS AND SYSTEM MODEL

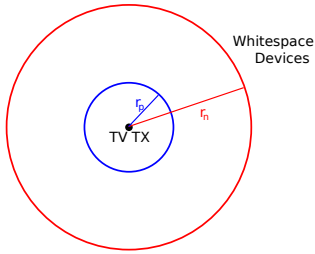


Fig. 1. Model setup: there is a TV transmitter at the origin, receivers within the protected radius  $r_p$ , no transmitters between  $r_p$  and  $r_n$ , and whitespace devices outside  $r_n$  with some placement distribution. In the Poisson model, these nodes are distributed as a 2D Poisson process with rate  $\lambda$ .

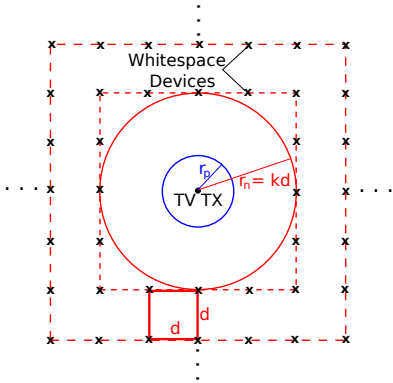


Fig. 2. Setup for the grid model. Outside  $r_n$ , whitespace devices are in a regular square grid, separated from each of their neighbors by  $d$ .  $r_n$  is assumed to be an integer multiple  $k$  of  $d$ .

The model setup is shown in Fig. 1. There is a TV transmitter at the origin, with receivers anywhere within the protected radius  $r_p$ . In this paper, for analytical simplicity, we assume that  $r_p = 0$ , so the primary transmitter and receiver are co-located at the origin.<sup>2</sup> All whitespace devices act like

<sup>2</sup>This is a corner case in that the interference seen at the receiver is worst when the receiver is at the origin with given  $r_n$ . This is compared to a receiver at  $r_p$  with  $r_n - r_p$  the same as the original  $r_n$ . In the first case, the closest interferers on all sides are equidistant to the receiver. In the second case, half the interferers are at approximately the same distance as before, and the others are much farther away.

interferers and are located outside a circle of the radius  $r_n$  from the origin. Each has power  $P$ . We assume a path-loss model in which the power observed at the origin from interferer  $j$  at a distance  $r_j$  is given by:

$$I_j(r_j) = XP r_j^{-\alpha} \quad (1)$$

where  $\alpha$  is the path-loss exponent, and  $X$  is the fading parameter. For all calculations with fading, we assume  $X \sim Exp(\mu)$ . We denote the total amount of interference seen at the origin from all the interferers as

$$I_T = \sum_j I_j(r_j). \quad (2)$$

We use two models for the distribution of the interferers. The *grid model* is shown in Fig. 2. The interferers lie on concentric squares around the origin, with distance  $d$  between an interferer and each of its neighbors. For simplicity, we assume the innermost square has minimum distance  $r_n = kd$  from the origin where  $k$  is an integer. Consistent with the Introduction, near field is when  $d \gg r_n$ , and far field is when  $d \ll r_n$ .

In the *Poisson model*, we assume that the interferers are randomly distributed as a 2D Poisson process [7] with rate  $\lambda$  everywhere outside of the radius  $r_n$ .

For all numerical calculations, we use the following parameter values:  $P = 1$ ,  $\alpha = 2.5$ ,  $\mu = 1$ ,  $d = 1$ . For space reasons, some of the proofs are omitted; they can be found in [16].

## III. NEAR VS FAR FIELD IN THE GRID MODEL

With the grid model and no fading, the interference seen at the origin is deterministic. In [10], the interference from a grid model with  $r_n = 0$  is computed analytically in an order sense. We use similar methods to calculate it for  $r_n \neq 0$ .

**Theorem 1:** For the grid model, with notation as in Section II, the total interference  $I_T$  is bounded by:

$$I_T \geq \frac{\eta P}{d^\alpha} \left( \frac{1}{k^{\alpha-1}} + \frac{1}{(\alpha-2)(k+1)^{\alpha-2}} \right), \quad (3)$$

$$I_T \leq \frac{\eta P}{d^\alpha} \left( \frac{1}{k^{\alpha-1}} + \frac{1}{(\alpha-2)k^{\alpha-2}} \right) \quad (4)$$

where  $8 \leq \eta \leq 8/2^{\alpha/2}$ .

*Proof:* See Appendix A. ■

These bounds are shown in Fig. 3. Notice that there are two distinct regions, where a different part of the expression dominates: when  $k$  is large, the interference power decays with  $r_n$  as  $r_n^{\alpha-2}$ . This is the same behavior of the sea model considered in [4]: the interferers are close enough together that an integral over their power density is a good approximation of the sum of the individual powers. In our model,  $k = 1$  is the lowest possible value. But, if  $k$  could be *very* small, the expression in Theorem 1 would be dominated by the  $1/k^{\alpha-1}$  term. Since we cannot make  $k$  that small, the slope in Fig. 3 is only  $-0.8$  in near field ( $k$  small).

If the propagation in a wireless environment were actually deterministic and interferers sat on a regular grid, this result shows a few things: first,  $d$ , the distance between interferers, acts *only* as a scaling factor. The behavior of the aggregate

interference instead depends on the *ratio* of  $r_n$  to  $d$ . Therefore, a rural environment, where would expect  $d$  to be at least comparable  $r_n$ , will exhibit very different behavior than an urban one with  $r_n$  large compared to  $d$ . How should this be accounted for?

Before tackling that question, we note that the propagation and interferer placement are never actually deterministic and on a regular grid. The next section discusses what happens when node placement is determined by the Poisson model.

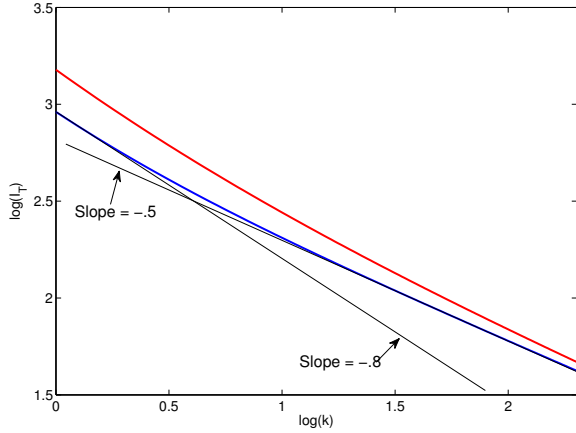


Fig. 3. Upper and lower bounds for the interference power from the grid model with  $\alpha = 2.5$ . Low  $k$  (near field) has a decay rate different from large  $k$  (far field). In far field, the decay rate agrees with that of a sea model [4] because the sum of the individual interferer powers is well approximated by an integral of the equivalent power density.

#### IV. NEAR VS FAR FIELD IN THE POISSON MODEL

In this section, we first focus on the shape of the interference distribution. We notice that while the mean and variance do not change, the shape changes from near to far field from a heavy-tailed distribution to something that is approximately Gaussian. We then numerically explore this approximate Gaussianity and how fast the distribution converges with a variational distance metric.

##### A. Form of the interference pdf

In the grid model, the behavior of the deterministic interference power was qualitatively different in near and far field, and only in far field did it behave like what we would expect from a sea. In the Poisson model, however, intuitively the mean interference power should not change. This is because there are no enforced holes between interferers, so the mean interference with a Poisson model should be well approximated with an integral regardless of near or far field.

**Theorem 2:** For a set of 2-D Poisson( $\lambda$ ) distributed interferers with minimum distance  $r_n$  from the point of measurement, the mean and variance of the total interference  $I_T$  is given by

$$E[I] = \frac{2\pi\lambda P}{(\alpha - 2)r_n^{\alpha-2}} \quad (5)$$

$$\text{var}[I] = \frac{2\pi\lambda P^2}{(2\alpha - 2)r_n^{2\alpha-2}} \quad (6)$$

*Proof:* See Appendix B. ■

Notice that the mean decreases with  $r_n$  as  $r_n^{\alpha-2}$ , and the standard deviation (square root of the variance) is decreasing as  $1/r_n^{\alpha-1}$ . Because the standard deviation is falling faster than the mean, the distribution is *concentrating* about the mean as  $r_n$  increases.

The mean and variance do not change behavior in near vs far field, but the *distribution* does. We find the distribution of the total interference power by numerically inverting the Laplace transform of the distribution from [7]:

**Theorem 3:** The Laplace Transform of the interference seen at a point from a set of interferers distributed as a 2D Poisson process with rate  $\lambda$  outside of a ring  $r_n$  from the point of observation is

$$L_I(t) = \exp(-\lambda 2\pi \int_{r_n}^{\infty} z(1 - e^{-Pt/z^\alpha}) dz) \quad (7)$$

*Proof:* See Corollary 2.3.2 in [7] with the Laplace Transform of the power from each interferer as

$$L_P(tP/z^\alpha) = e^{-tP/z^\alpha} \quad (8)$$

because there is no fading, so the CDF is a step function at the power of the interference with path loss. ■

Fig. 4 shows the pdf for several values of  $\lambda$ , keeping  $r_n$  fixed at one. The means of these distributions are growing because we are just increasing the density of nodes. Furthermore, for smaller values of  $\lambda$  (closer to near field), the distribution has a heavier tail and when  $\lambda$  grows, the distribution more resembles a Gaussian.<sup>3</sup> This is not surprising: as the nodes get closer together, they each contribute a similar amount of interference to the total. They are also larger in number. So, some version of the Central Limit Theorem is likely to apply. Next, we use the variational distance to Gaussian to numerically explore near vs far field.

##### B. Convergence to a Gaussian

We choose the metric of variational distance ( $L_1$  norm of the difference between the pdf's) to track the convergence to Gaussian because it is scale invariant.<sup>4</sup> Scale invariance is important because as we change  $r_n$  and  $\lambda$ , the mean and variance of the distribution change, so the distribution is scaled and shifted. However, it is possible to draw contours in the  $(r_n, \lambda)$ -space where the variational distance to Gaussian does *not* change. These contours are shown in Fig. 5. Our work with the grid model suggests that these contours of equal variational distance should exist: if the distance is invariant to the scaling factor ( $d$  for the grid), the only determining factor is  $k$ , the

<sup>3</sup>The heavy tail in near field was noticed also in [8]

<sup>4</sup>Given  $X$  and  $Y$  with PDFs  $f_X(x)$ ,  $f_Y(y)$ , and some positive scaling factor  $m$ :

$$\begin{aligned} d(mX, mY) &= \int \left| \frac{1}{m} f_X(mx) - \frac{1}{m} f_Y(mx) \right| dx \\ &= \int \left| \frac{1}{m} f_X(t) - \frac{1}{m} f_Y(t) \right| m dt \\ &= |f_X(t) - f_Y(t)| dt \\ &= d(X, Y) \end{aligned}$$

ratio of  $r_n$  to  $d$ . For the Poisson model, the distance between interferers is a probabilistic function of  $\lambda$ . There should be a function of  $r_n$  and  $\lambda$  that serves the same function as  $k$ .

The shape of the contours can be understood through a thought experiment: Choose an  $r_n$  and  $\lambda$ , and fix a realization. Then, zoom in on this realization so that  $r_n$  grows and the interferers spread out. The probability that the interferers fall in small balls around their current positions (and therefore cause approximately the same interference) is the same for the original and zoomed-in situations. The only thing that has changed is the total interference caused by the interferers, because they are now closer to the origin. Considering all the possible positions of the interferers, the resulting pdf has been shifted and scaled, but has not has not changed its variational distance from the corresponding Gaussian that has been shifted and scaled in the same way.

To be more concrete, if we zoom in such that  $r_n$  has changed by  $1/m$ , then the density of interferers has changed by  $1/m^2$ , and therefore  $\lambda$  has changed by  $m^2$ . The total interference, originally  $I_T = \sum_j \frac{P}{r_j^\alpha}$  has changed to  $I_T = m^2 \sum \frac{P}{(r/m)^\alpha}$ . Therefore, the sets of points  $(r_n/m, m^2\lambda)$ , for all  $m$  define the contours. As an equation, the contours are defined by  $r_n^2\lambda = c$  where  $c$  is a constant.

These equivalence classes are very useful: some values of  $r_n$  and  $\lambda$  are numerically more difficult to evaluate than others, but only one is required to be evaluated for the whole class and the actual distribution can be found by scaling and shifting the result. Also, by looking at the  $r_n$  and  $\lambda$  for any given real world situation, the government regulator can tell whether they need to define  $r_n$  to account for a heavy tailed distribution or a Gaussian distribution. Further, if the real parameters are in far field, the Gaussian approximation is good and much simpler than trying to work with the actual distribution.

Fig. 6 shows how quickly the distribution converges to Gaussian as  $r_n^2\lambda$  grows. We find by visual inspection that the variational distance follows the relationship  $(r_n^2\lambda)varDist^{1/\delta} = c$ , where  $c$  is a constant (when plotted on a log-log scale, the sum of these two terms is a constant, so  $\delta$  is the slope of Fig. 6). For our case here with no fading and  $\alpha = 2.5$ ,  $\delta \approx -1$ .

Adding the random Poisson distribution of placement significantly affected the behavior in near and far field. Will a similarly significant change result from adding fading, another source of randomness in any real system? We explore this next.

## V. THE EFFECT OF FADING

For the grid, adding fading will create a distribution where before it was deterministic. But, if we assume the mean of the fading is one, the mean of the interference power does not change. Therefore, the difference between near and far field can still be viewed through the mean.

For the Poisson model, we can calculate the mean and variance with fading:

**Theorem 4:** For a set of 2-D Poisson-distributed interferers of density  $\lambda$  with minimum distance  $r_n$  away from the point of measurement, each with exponential fading parameter  $X_i \sim Exp(\mu)$ , the mean and variance of the total interference  $I$  is

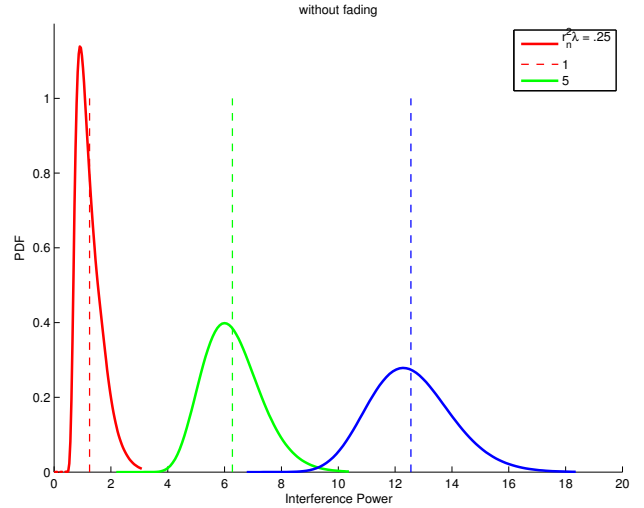


Fig. 4. pdf of the power of the interference in the Poisson model without fading, holding  $r_n = 1$  and changing  $\lambda = 0.25, 1, 5$ . The mean power increases due to the larger density of nodes. The shape of the distribution also changes: for lower  $\lambda$  (near field) there are heavy tails. For larger  $\lambda$  (far field), the distribution resembles a Gaussian.

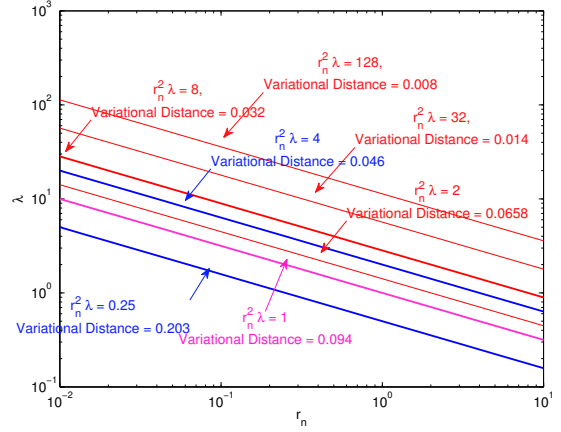


Fig. 5. The variational distance between the interference distribution and the appropriate Gaussian without fading.  $\alpha = 2.5$

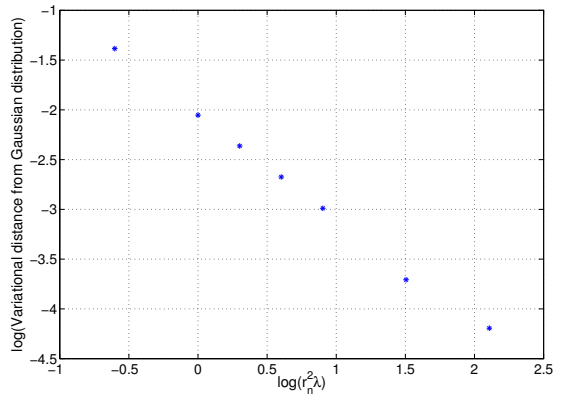


Fig. 6. Variational distance by  $\lambda r_n^2$  without fading and with  $\alpha = 2.5$ . The slope is approximately  $-1$ .

given by:

$$E[I] = \frac{2\pi\lambda P}{\mu(\alpha - 2)(r_n)^{\alpha-2}} \quad (9)$$

$$\text{var}[I] = \frac{4\pi\lambda P^2}{\mu^2(2\alpha - 2)r_n^{2\alpha-2}} \quad (10)$$

where  $P$  is the power of each interferer, and  $\alpha$  is the path-loss exponent.

*Proof:* See Appendix C. ■

If we assume  $\mu = 1$ , the mean of the distribution does not change. However, the variance doubles. The factor of 2 is an effect of choosing the Exponential distribution for the fading, and may not extend to other models. More importantly, how does the distribution change with fading? We can again find the Laplace transform of the total interference with [7]:

**Theorem 5:** The Laplace Transform of the interference seen at a point from a set of interferers distributed as a 2D Poisson process with rate  $\lambda$  outside of a ring  $r_n$  from the point of observation with  $\text{Exp}(\mu)$  fading is

$$L_I(t) = \exp\left(-\lambda \int_0^{2\pi} \int_{r_n}^{\infty} \frac{ztP}{Pt + \mu z^\alpha} dz d\theta\right) \quad (11)$$

*Proof:* See Corollary 2.3.2 in [7] with the Laplace Transform of the power from each interferer as

$$L_P(tP/z^\alpha) = \frac{\mu}{Pt/z^\alpha + \mu} \quad (12)$$

because the fading is exponential. ■

Fig. 7 shows the pdf for  $r_n = 1$  and several values of  $\lambda$ . Notice that the tails are larger here than they were without fading, so the fading is exaggerating the near field effect. It also seems to be slowing the transition to a Gaussian distribution. However, the transition to Gaussian is still occurring. Fig. 8 shows the rate of convergence to Gaussian compared to the case without fading.

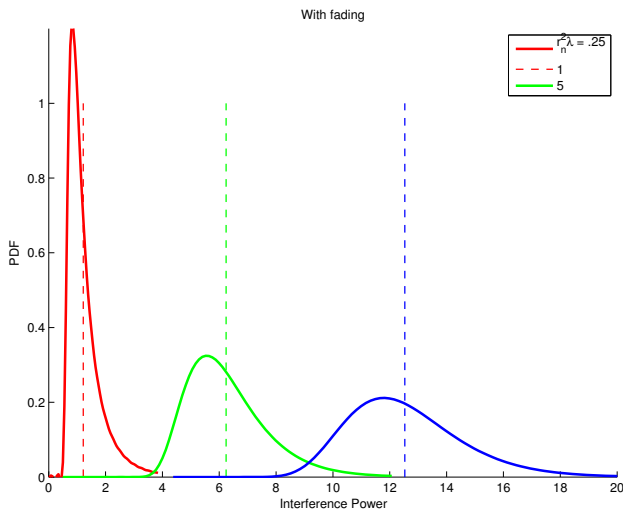


Fig. 7. pdf of the interference distribution with exponential fading,  $r_n = 1$ ,  $\lambda = 0.25, 1, 5$ . As shown in Section V, the variance of the distribution doubles because of exponential fading. The convergence to Gaussian also slows.

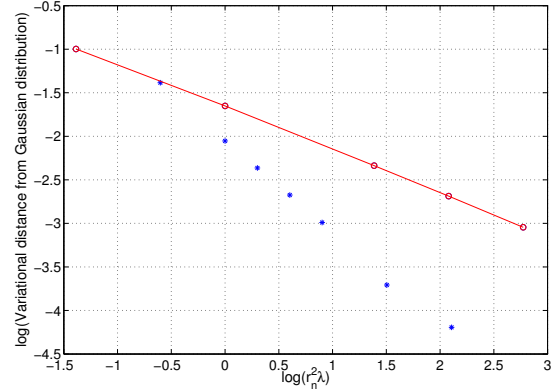


Fig. 8. Blue points are the same as in Fig. 6 and have no fading. The red points and line show the variational distance to Gaussian with exponential fading. With fading the convergence slows: the slope is now approximately  $-1/2$ .

## VI. CONCLUDING REMARKS

In this paper, we have investigated the behavior of aggregate interference with a grid and Poisson model for placement of whitespace devices. We find that in near and far field, the behavior can be very different. In the (deterministic placement) grid model, unlike the prediction of the sea-model, the decay of the observed interference falls with  $r_n$  changes depending on whether we are operating in near field or far field. For the (random-placement) Poisson model, the interference in near field exhibits a heavy tail distribution; in far field, the distribution is approximately Gaussian. Additional randomness introduced by fading does not change the qualitative behavior. However, the variance of the interference increases and the rate of convergence to Gaussian decreases.

These results could be useful for designing power rules: if we know the relevant parameters ( $r_n$  and  $\lambda$ ), we know whether the distribution of interference will look heavy-tailed or Gaussian (depending on the value of  $r_n^2\lambda$ ). When it looks Gaussian (*i.e.* when  $r_n^2\lambda \gg 1$ ), it is easy to choose the right  $r_n$  and power limit to ensure a maximum outage probability of primary transmissions. Even when we are operating in near-field, when the interference does not look Gaussian, our results give an idea of the heavy tail the regulator is facing. We leave for future work getting simple bounds on these tails so that even in near field, the required calculations to define the rules are simple.

But is near field actually a relevant operating situation? Consider the following scenario:  $r_n$  is 14.4 km. Our results suggest that  $r_n^2\lambda > 1$  suffices for a reasonable Gaussian approximation. In this case,  $\lambda$  must be less than  $1/200,000$  per sq km or the density of nodes must be less than one node per 200 sq km to be in near field. If we are in a rural scenario, and the nodes are actually ISP towers, this density is reasonable. With fading exaggerating near field, the required density can occur even more easily. Knowing how to deal with near field is therefore important. Further, our results are not limited to the TV band; in a band where the primary and secondary devices are of similar powers, they may have similar MAC exclusion

requirements which will create a near field situation.

Furthermore, understanding the difference between near and far field will help future work in understanding whether a “one-size-fits-all” power rule is sufficient: it must be designed for the worst case. But if the worst case causes significant degradation on the best case, perhaps rules designed for specific usage scenarios or rules based on more than  $r_n$  and a power limit will be required (this question was addressed in [3] for a deterministic model).

Finally, this work should be extended to relax the assumptions. In particular, the case of primary receivers that are not co-located with their transmitters ( $r_p \neq 0$ ) should be explored. It is also important to understand what happens when MAC protocols are used by cognitive transmitters in order to improve their performance by introducing some minimum separation between cognitive transmitters [7]. The spatial correlation induced by MAC protocols is mathematically hard to handle, and in far field has been successfully approximated by Poisson distribution [7]. Because near-field is an interesting regime for our practical setup, the spatial-correlations need to be understood. Recent results from [17] could help obtain some insights for these problems.

#### APPENDIX A PROOF OF THEOREM 1

Assume a grid model, with  $r_n = kd$ . Each node is shared between four squares of area  $d^2$ , each of which has four nodes at its corners. Therefore  $1/d^2$  is the density of nodes. We take  $i$  as the index of each successive square of nodes around the receiver, and  $k$  as the center-most square of nodes. Note (see Fig. 2) that square  $i + 1$  has 8 more interferers than square  $i$ , and the innermost square has  $8k$  nodes. We bound the total interference by putting all nodes on a circle at the smallest distance to the center and at the longest distance to the center in any particular square (these differ by  $\sqrt{2}$ ):

$$\sum_{i=0}^{\infty} \frac{8P(k+i)}{(d(k+i))^\alpha} \geq I_T \geq \sum_{i=0}^{\infty} \frac{8P(k+i)}{(\sqrt{2}d(k+i))^\alpha} \quad (13)$$

$$\Rightarrow \frac{8P}{d^\alpha} \sum_{i=0}^{\infty} \frac{1}{(k+i)^{\alpha-1}} \geq I_T \geq \frac{8P}{(\sqrt{2}d)^\alpha} \sum_{i=0}^{\infty} \frac{1}{(k+i)^{\alpha-1}} \quad (14)$$

Because the upper and lower bound differ by a factor of  $2^{\alpha/2}$ , the total interference is:

$$I_T = \frac{\eta P}{d^\alpha} \sum_{i=0}^{\infty} \frac{1}{(k+i)^\alpha} \quad (15)$$

for some  $8 \geq \eta \geq 8/2^{\alpha/2}$ . Then, we can bound the sum with integrals by taking the integral above and below the stair-case function that defines the sum (functionally, the difference is that the upper bound integral begins at  $k + 1$ , and lower bound

at  $k$ ):

$$I_T \geq \frac{\eta P}{d^\alpha} \left( \frac{1}{k^{\alpha-1}} + \int_{k+1}^{\infty} \frac{1}{x^{\alpha-1}} dx \right) \quad (16)$$

$$= \frac{\eta P}{d^\alpha} \left( \frac{1}{k^{\alpha-1}} + \frac{1}{(\alpha-2)(k+1)^{\alpha-2}} \right), \quad (17)$$

$$I_T \leq \frac{\eta P}{d^\alpha} \left( \frac{1}{k^{\alpha-1}} + \int_k^{\infty} \frac{1}{x^{\alpha-1}} dx \right) \quad (18)$$

$$= \frac{\eta P}{d^\alpha} \left( \frac{1}{k^{\alpha-1}} + \frac{1}{(\alpha-2)k^{\alpha-2}} \right) \quad (19)$$

#### APPENDIX B PROOF OF THEOREM 2

Divide the space into concentric annuli of width  $dr$ , starting from  $r_n$ . Let  $r_j$  be the distance from the center to annulus  $j$  and  $N_j \sim Poiss(\lambda 2\pi r_j dr)$  be the number of nodes in annulus  $j$ . Then

$$E[I_T] = E \left[ \sum_{j=1}^{\infty} \sum_{i=1}^{N_j} \frac{P}{r_j^\alpha} \right] \quad (20)$$

$$= \sum_{j=1}^{\infty} \frac{P}{r_j^\alpha} E[N_j] \quad (21)$$

$$= \sum_{j=1}^{\infty} \frac{P}{r_j^\alpha} \lambda 2\pi r_j dr \quad (22)$$

$$= \int_{r_n}^{\infty} \frac{2\pi r \lambda P}{r^\alpha} dr \quad (23)$$

$$= \frac{2\pi \lambda P}{(\alpha-2)r_n^{\alpha-2}} \quad (24)$$

Using the same division of space into annuli:

$$var[I_T] = var \left[ \sum_{j=1}^{\infty} \sum_{i=1}^{N_j} \frac{P}{r_j^\alpha} \right] \quad (25)$$

$$= var \left[ \sum_{j=1}^{\infty} \frac{N_j P}{r_j^\alpha} \right] \quad (26)$$

$$= \sum_{j=1}^{\infty} \frac{P^2}{r_j^{2\alpha}} var[N_j] \quad (27)$$

$$= \sum_{j=1}^{\infty} \frac{P^2}{r_j^{2\alpha}} 2\pi r_j dr \lambda \quad (28)$$

$$= 2\pi \lambda P^2 \int_{r_n}^{\infty} r^{1-2\alpha} dr \quad (29)$$

$$= \frac{2\pi \lambda P^2}{(2\alpha-2)r_n^{2\alpha-2}} \quad (30)$$

APPENDIX C  
PROOF OF THEOREM 4

$$E[I] = E \left[ \sum_{j=1}^{\infty} \sum_{i=1}^{N_j} \frac{X_i P}{r_j^\alpha} \right] \quad (31)$$

$$= \sum_{j=1}^{\infty} E[N_j] E[X_i] \frac{P_2}{r_j^\alpha} \quad (32)$$

$$= \frac{2\pi\lambda P_2}{\mu(\alpha - 2)r_n^{\alpha-2}} \quad (33)$$

$$\text{var}[I] = \text{var} \left[ \sum_{j=1}^{\infty} \sum_{i=1}^{N_j} \frac{X_i P}{r_j^\alpha} \right] \quad (34)$$

$$= \sum_{j=1}^{\infty} \frac{P_2^2}{r_j^{2\alpha}} \text{var} \left[ \sum_{i=1}^{N_j} X_i \right] \quad (35)$$

$$= \sum_{j=1}^{\infty} \frac{P_2^2}{r_j^{2\alpha}} \left[ \lambda A \frac{1}{\mu^2} + \lambda A \frac{1}{\mu^2} \right] \quad (36)$$

$$= \frac{4\pi\lambda P_2^2}{\mu^2(2\alpha - 2)r_n^{2\alpha-2}} \quad (37)$$

REFERENCES

- [1] "In the matter of unlicensed operation in the tv broadcast bands: Second report and order and memorandum opinion and order.," Tech. Rep. 08-260, Federal Communications Commission, Nov. 2008.
- [2] "In the matter of unlicensed operation in the tv broadcast bands: Second memorandum opinion and order," Tech. Rep. 10-174A1, Federal Communications Commission, Sept. 2010.
- [3] K. Harrison and A. Sahai, "Potential collapse of whitespaces and the prospect for a universal power rule," *Proceedings of the Fifth IEEE International Symposium on New Frontiers in Dynamic Spectrum Access Networks*, May 2011.
- [4] N. Hoven and A. Sahai, "Power scaling for cognitive radio," *International Conference on Wireless Networking, Communications, and Mobile Computing*, June 2005.
- [5] M. Vu, N. Devroye, and V. Tarokh, "The primary exclusive region in cognitive networks," *Consumer Communications and Networking Conference, 2008. CCNC 2008. 5th IEEE*, pp. 1014 – 1019, Jan. 2008.
- [6] T. V. Nguyen and F. Baccelli, "A probabilistic model of carrier sensing based cognitive radio," in *New Frontiers in Dynamic Spectrum (DySPAN), IEEE Symposium on*, (Singapore), April 2010.
- [7] F. Baccelli and B. Blaszczyszyn, "Stochastic geometry and wireless networks." URL for Volume I: <http://hal.inria.fr/inria-00403039> and for Volume II: <http://hal.inria.fr/inria-00403040>, 2009. To appear in *Foundation and Trend in Networking*, NOW publisher.
- [8] T. V. Nguyen and F. Baccelli, "Interference from cognitive radio device," *Submitted to DySPAN 2011*, 2011.
- [9] T. Valone, *Harnessing the Wheelwork of Nature: Tesla's Science of Energy*. Adventures Unlimited Pr, 2002.
- [10] M. Haenggi and R. K. Ganti, "Interference in large wireless networks," *Foundations and Trends in Networking*, no. 2, pp. 127–248, 2009.
- [11] M. Haenggi, J. Andrews, F. Baccelli, O. Dousse, and M. Franceschetti, "Stochastic geometry and random graphs for the analysis and design of wireless networks," *Selected Areas in Communications, IEEE Journal on*, vol. 27, no. 7, pp. 1029–1046, 2009.
- [12] J. Andrews, F. Baccelli, and R. Ganti, "A Tractable Approach to Coverage and Rate in Cellular Networks," *Arxiv preprint arXiv:1009.0516*, 2010.
- [13] K. Huang and J. Andrews, "A Stochastic-Geometry Approach to Coverage in Cellular Networks with Multi-Cell Cooperation," *Arxiv preprint arXiv:1103.4223*, 2011.
- [14] M. Alouini and A. Goldsmith, "Area spectral efficiency of cellular mobile radio systems," *Vehicular Technology, IEEE Transactions on*, vol. 48, no. 4, pp. 1047–1066, 1999.

- [15] D. Tse and P. Viswanath, *Fundamentals of Wireless Communications*. Cambridge University Press, 2005.
- [16] <http://www.eecs.berkeley.edu/~kwoyach/papers/globecom11Extended.pdf>.
- [17] R. Ganti, F. Baccelli, and J. Andrews, "Series Expansion for Interference in Wireless Networks," *Arxiv preprint arXiv:1101.3824, Submitted to IEEE Trans. Inform. Theory*, 2011.